SNS INJECTION AND EXTRACTION SYSTEMS – ISSUES AND SOLUTIONS*

M Plum, Oak Ridge National Laboratory, Oak Ridge, TN, USA

Abstract

Beam loss is higher than expected in the Ring injection section and in the injection dump beam line. The primary causes are fairly well understood, and we have made some equipment modifications to reduce the loss. In the ring extraction beam line the beam distribution exhibits cross-plane coupling (tilt), and the cause has been traced to a large skew-quadrupole component in the extraction Lambertson septum magnet. In this paper we will discuss the issues surrounding the ring injection and extraction systems, the solutions we have implemented to date, and our plans for future improvements.

INTRODUCTION

Beam commissioning of the HEBT, Ring, and RTBT began in January 2006, and since that time the majority of the HEBT, Ring, and RTBT systems have performed very well. The ring design team deserves a lot a credit for their good work. However, several issues concerning the Ring injection and extraction have come to light, and this paper reports on the status of these issues.

INJECTION

To inject beam into the ring, H^- beam from the linac is charge-exchange injected using a 0.30 mg/cm^2 carbon stripper foil located inside the second chicane magnet of a four-chicane orbit bump, as shown in Fig. 1. Beam that is stripped to H^+ begins to circulate around the ring. Beam that is partially stripped to H^0 either field-strips to H^+ or stays as H^0 and is intercepted by a secondary stripper foil, where it is converted to H^+ and directed to the beam dump. Some of the injected H^- beam misses the foil by design, and this beam is also intercepted by the same secondary foil, converted to H^+, and directed to the beam dump. Both these beams are positive polarity after the secondary stripper foil, but for clarity we label the H^- beam that misses the foil as the H^- waste beam, and the partially stripped H^0 beam as the H^0 waste beam.

This area of the ring is has the most complicated beam optics of the entire accelerator complex. Many constraints must be simultaneously satisfied: (a) the circulating beam displacement of four-chicane closed orbit bump is about 100 mm, (b) the H^- and circulating beams are merged with a relative angle of zero, (c) the magnetic field at the foil is 2.5 kG, and the field in the third chicane magnet is <2.4 kG, to control the H^0 excited states, (d) the field tilt [arctan(By/Bz)] at the foil is >65 mrad to keep the stripped electrons off the foil and funnel them down to a water-cooled electron catcher, and (e) the H^- and H^0 waste beams are transported to the beam dump.

During the early days of commissioning we discovered that the four-chicane bump was not functioning according to the design. We traced the cause to a design change made to the second and third chicane magnets [1] that was not fully appreciated at the time, which caused poor injection into the ring and poor transmission of the H^- and H^0 waste beams. We were able to adjust the magnetic fields in all four chicane magnets to give good injection into the ring, but there is no solution that gives both good injection and good transmission of the waste beams to the dump. Consequently the beam loss in the injection dump beam line was very high, and only one of the two waste beams could be transported to the dump.

Another issue in the ring injection area is that the original design did not include a method to independently control the H^0 and H^- waste beams. Both beams passed through all the same magnets, so they could not be separately optimized.

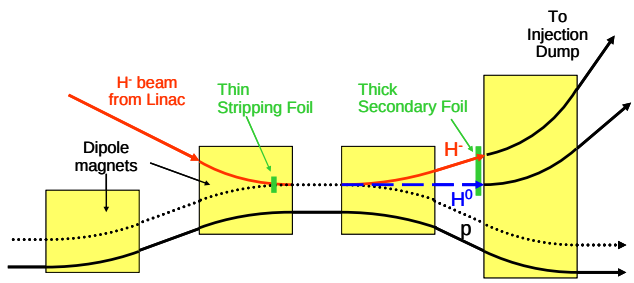

Fig. 1. A schematic diagram of the ring injection chicane.

The third issue in the injection area is the measurement of the beam distributions and positions at the dump. The dump is rated for 150 kW of beam power, and with this much power it is very important to know where the beams hit the dump and what their distributions are. However, the last beam diagnostic is a wire scanner located 12.6 m upstream of the dump. The next-closest diagnostic is a beam position monitor (BPM) located 19.9 m upstream of the dump. We now estimate beam positions by extrapolating measured positions at this wire scanner and BPM down to the dump, and we estimate the beam distributions from model calculations. But these methods are indirect and an easier, faster, more direct, and more accurate method is clearly desirable.

Injection dump beam line modifications

The first modification, in June 2006, illustrated in Fig. 2, was to increase the width of the secondary stripper foil to allow a wider range of chicane magnet settings while still intercepting the H^- waste beam. Since the secondary foil was already as wide as a single foil could

* ORNL/SNS is managed by UT-Battelle, LLC, for the U.S. Department of Energy under contract DE-AC05-00OR22725

be and still fit through the vacuum port, a two-part hinged foil was designed that could be folded into a smaller shape to pass through the vacuum port, and then expand once it is inside the vacuum vessel.

The next modification, in November 2006, was to replace the ~0.3 mg/cm^2, 12 x 40 mm^2 primary stripper foil with a wider, thicker, ~0.45 mg/cm^2, 17 x 40 mm^2 foil. The wider foil intercepted almost 100% of the incoming H^- beam, thus reducing the number of waste beams from two to one, and allowing the injection dump beam line to be set to transport just the H^0 waste beam. Since the foil was also thicker, the H^0 waste beam intensity was also reduced. The unfortunate consequence of this change was to increase the beam losses due to the circulating beam scattering in the foil.

A number of additional modifications were made in April-May 2007. The fourth chicane magnet was shifted 8 cm beam left, a C-magnet was installed just downstream of the injection dump septum magnet, and new beam diagnostics were installed just downstream of the C-magnet (a beam position monitor, a wire scanner, and a high-sensitivity beam current monitor).

The fourth chicane magnet was shifted 8 cm beam left because we discovered [2] that the H^- waste beam was passing outside the good field region of the magnet, causing a vertical deflection large enough to create unacceptable beam loss in the injection dump beam line.

The C-magnet was added just downstream of the injection dump septum magnet to allow independent control over the horizontal steering of the two waste beams. The field of this magnet primarily steers just the H^- waste beam.

In March 2008, we replaced the injection dump gradient septum magnet with a modified version of the spare septum magnet. This new magnet has a gap 2 cm larger than the original, thus increasing the vertical aperture of the magnet to further reduce beam losses. The vacuum chamber within the magnet was also modified to make better use of both the horizontal and vertical aperture of the magnet. [3]

The most recent modification was to replace the secondary stripper foil. Even before commissioning the ring we knew the original 25 mg/cm^2 carbon-carbon was thicker than desirable. Ideally the thickness would be just 1 mg/cm^2, but other constraints, such as the large size and the requirement that the foil be self supporting, have so far prevented us from reaching this goal. The thinnest carbon-carbon foil we could find is the 18 mg/cm^2 thick foil by Allcomp, but this was also too thick, and, like the original carbon-carbon foil, it developed pinholes after several weeks of usage. In August 2008 we installed a 3.2 mg/cm^2 polycrystalline graphite foil. The improvements due to the thinner foil will be detailed next.

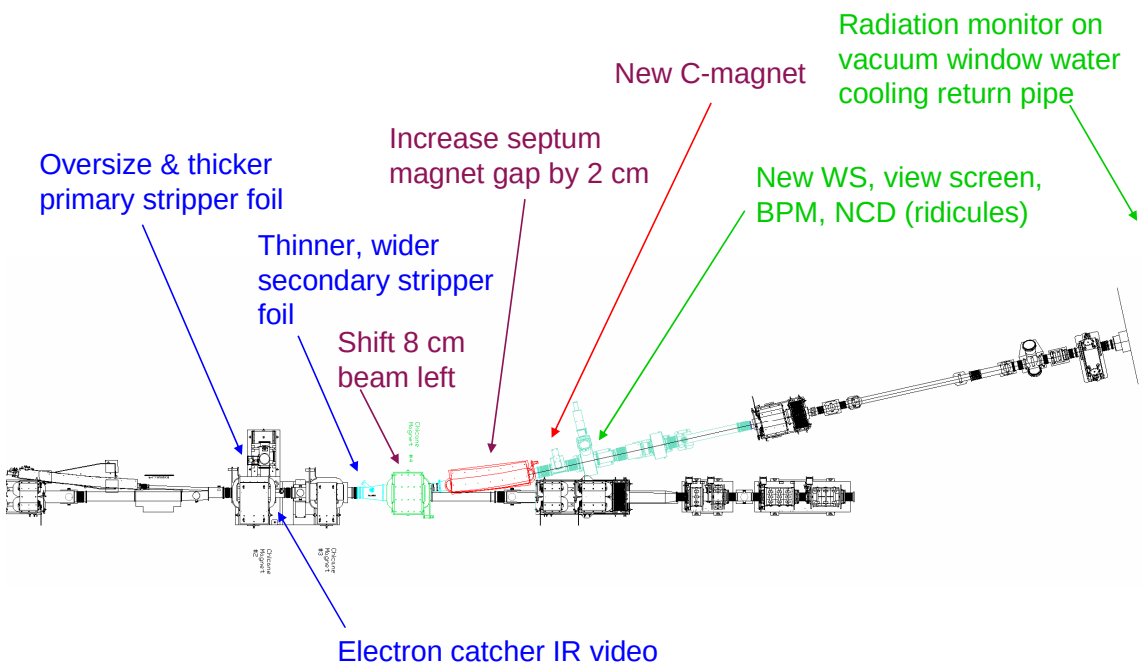

Fig. 2. Schematic diagram of ring injection area and the first part of the injection dump beam line, showing the various modifications that have been made since the start of commissioning.

Scattering in the secondary foil

A significant fraction of the beam loss in the injection dump beam line is due to scattering in the secondary foil. To quantify this loss, we made a series of beam loss measurements with the secondary foil inserted, and then after replacing the foil with the 1-mm thick chromium-doped aluminum-oxide view screen that is mounted to the same actuator mechanism. Most of the scattering of interest is large angle Rutherford scattering. A convenient

expression [4] for the probability that a particle will be Rutherford scattered outside of a given set of horizontal and vertical angles θ_{xl} and θ_{yl} is

$$P = \left(\frac{2Zm_e r_e}{\gamma M\beta^2}\right)^2 N_0\left(\frac{\rho t}{A}\right)\left[\frac{1}{\theta_{xl}\theta_{yl}} + \frac{1}{\theta_{xl}^2}\tan^{-1}\left(\frac{\theta_{yl}}{\theta_{xl}}\right) + \frac{1}{\theta_{yl}^2}\tan^{-1}\left(\frac{\theta_{xl}}{\theta_{yl}}\right)\right]$$

where Z is the charge number of the target nucleus, m_e and r_e are the electron's mass and classical radius, M is the mass of the incident particle, γ and β are the usual relativistic factors, ρt is the thickness of the target, A is the atomic mass of the target, and N_0 is Avogadro's number.

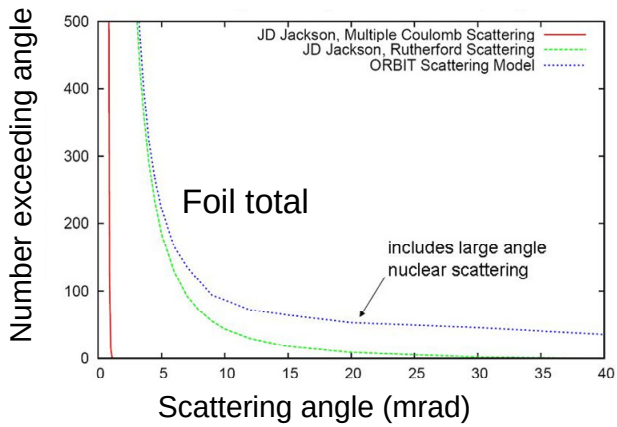

Fig. 3. ORBIT calculation [5] of beam scattering by the 18 mg/cm^2 secondary stripper foil, showing the different components that make up the total scattering. One million particles are launched, and the vertical axis indicates how many of these are scattered outside of a given angle.

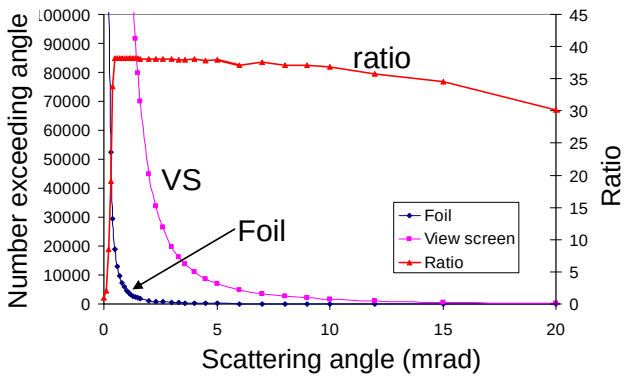

Fig. 4. ORBIT calculation [5] of beam scattering by both the 18 mg/cm^2 secondary stripper foil and the 1-mm thick view screen. One million particles are launched, and the vertical axis indicates how many of these are scattered outside of a given angle. The ratio of the two curves is also shown.

In this equation, the terms to the left of the square brackets depend only on the scattering target (foil or view screen). The terms within the brackets depend only on the scattering angles. This means that by substituting one target for another, any change in beam loss will be due to just scattering. If we express the beam loss as a sum of the base loss (e.g. beam halo) plus the loss due to scattering, with two scattering targets we have two measurements and two unknowns and we can determine the magnitudes of the losses due to each of the two components.

Of course the scattering is not completely due to Rutherford scattering. There is also multiple Coulomb and nuclear scattering. We have used the ORBIT accelerator modeling code, which includes all these effects, to compute the probability of a particle scattering outside a given aperture, and the result is shown in Figs. 3 and 4. These figures show that over our angular range of interest (about 3 to 10 mrad), the scattering is in fact dominated by Rutherford scattering, but more importantly, even after including large angle nuclear scattering, the ratio of foil scattering to view screen scattering is quite constant from less than 1 mrad up to about 10 mrad. This is exactly what we need to make this measurement.

Figure 5 shows the signals from beam loss monitors (BLMs) spaced along the injection dump beam line for two different cases – secondary foil inserted, and view screen inserted. The figure also shows the ratio of the two measurements. The ratio has a fairly constant value of 50 for all the BLMs, indicating that the beam loss caused by scattering in the view screen dominates the other sources of loss.

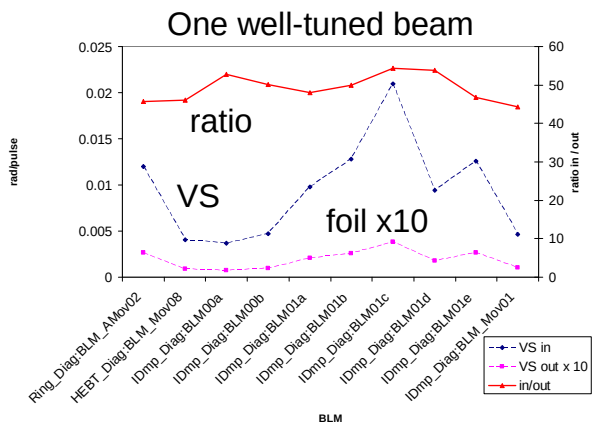

Fig. 5. Signal levels from beam loss monitors spaced along the injection dump beam line, for the case of one well-tuned (to minimize the beam loss) beam in the injection dump. Two cases are shown: secondary stripper foil inserted, and view screen inserted.

Figure 6 shows the a similar measurement for a simulated H^0 beam, where we remove the primary foil from the path of the incoming beam and adjust the magnetic fields to cause the beam to take the same path as the real H^0 beam under production conditions. The ratio now varies between 15 and 45, indicating that at the beginning of the injection dump beam line the loss due to scattering in the secondary foil is as high as 90%, and at the end of the beam line, where the ratio is 15, only 30% of the beam loss is due to scattering in the secondary foil. Due to the small size of the view screen, we are not able to make this type of a measurement for the simulated H^-

beam or the production beam, but we expect the numbers would be similar. Clearly, a thinner foil will give a significant improvement in beam losses.

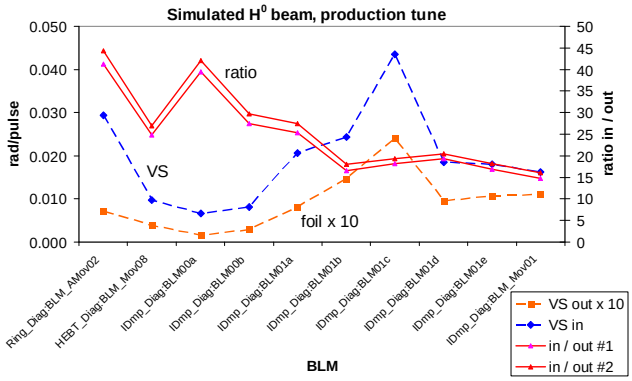

Fig. 6. Signal levels from beam loss monitors spaced along the injection dump beam line, for the case of the simulated H^0 beam. Two cases are shown: the 18 mg/cm^2 secondary stripper foil inserted, and the view screen inserted. The ratio of the two curves is also shown, for two cases to indicate the shot-to-shot repeatability.

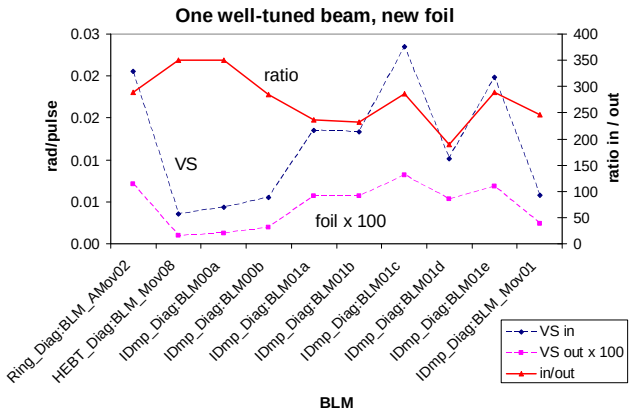

Fig. 7. Signal levels from beam loss monitors spaced along the injection dump beam line, for the case of the simulated H^0 beam. Two cases are shown: the new 3.2 mg/cm^2 secondary stripper foil inserted, and the view screen inserted. The ratio of the two curves is also shown.

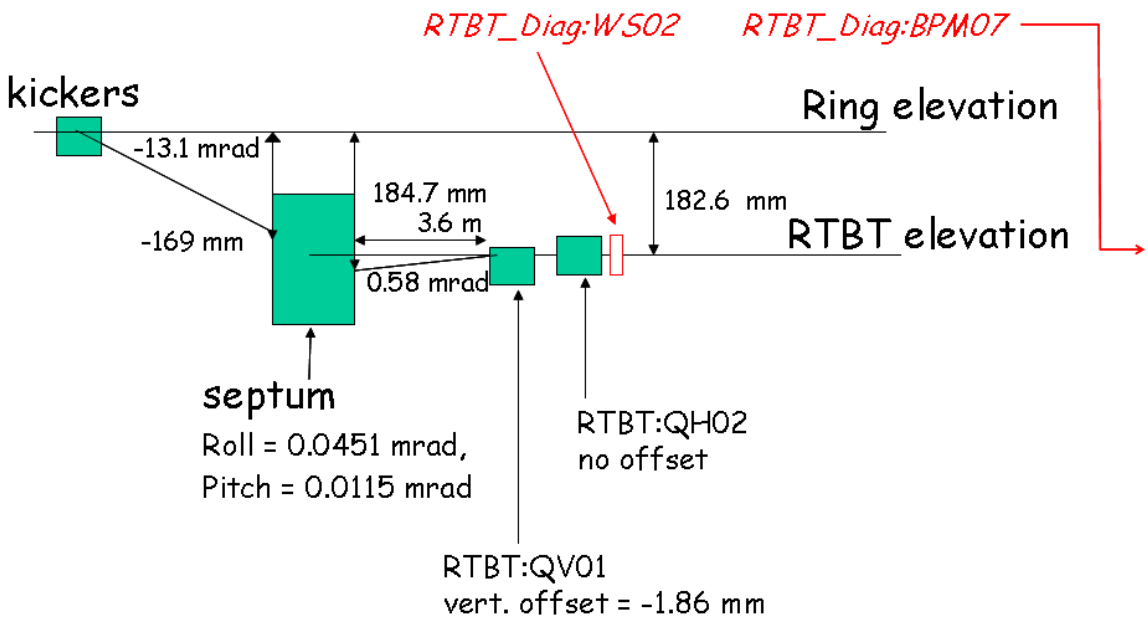

Fig. 8. Schematic diagram of the ring extraction area [6], showing the location of the first diagnostics in the RTBT extraction line.

As we mentioned earlier, in August 2008 we installed a thinner secondary foil (3.2 mg/cm^2 vs. 18 mg/cm^2), and we then repeated the measurement, shown in Fig. 7. The ratio for a well tuned beam is now approximately 300, which indicates that the loss due to scattering is now six times less than before, as expected for a foil that is six times thinner.

Questions and answers

Before the start of this workshop, the working group conveners posed three questions. The answers together with the questions follow for the case of the injection portion of the SNS ring.

Q1: Does the system perform as expected? Did the simulations/calculations performed during the design stage accurately predict the actual performance?

A1: No. The design bend angles of the chicane magnet set points were not correct. Beam loss in injection dump beam line was much higher than expected. Vertical deflection in chicane #4 was not expected.

Q2: What are the major limitations in performance? Were they known in the design stage?

A2: Beam loss in the injection dump beam line. This was not known in the design stage.

Q3: If someone were to begin now designing the same type of system for a similar machine, what is the one piece of advice that you would give them?

A3: 3-D field simulations and tracking in complex regions such as injection area are important. Map magnets well enough to determine higher order multipoles, for a wide range of currents. Allow independent control over multiple beams.

EXTRACTION

Extraction from the SNS ring is initiated by simultaneously firing a bank of 14 extraction kickers. The beam is deflected down into a Lambertson septum magnet, reaching a displacement of 169 mm and angle of 13.1 mrad at the entrance to the magnet, as shown in Fig. 8.

The septum magnet primarily deflects the beam to the left, but since it is rolled 0.0451 mrad, it also changes the incoming downward angle to a slight upward angle of 0.58 mrad. The first quadrupole magnet in the RTBT extraction line is offset 1.86 mm to cancel this upward angle and bring the extracted beam onto the elevation of the extraction beam line (182.6 mm below the elevation of the circulating beam).

The primary issues in the SNS ring extraction area are 1) tilted beam (cross plane coupling), 2) lack of diagnostics to measure the beam path in the ring and first 27 m of the RTBT, and 3) lack of beam profile and position info at the vacuum window and target.

Tilted beam

The tilted beam was first observed during the early stages of ring commissioning, when a temporary view screen installed on the front face of the mercury spallation target showed a beam image with a clear tilt. A representative image [1] is shown in Fig. 9.

More evidence was observed later, during benchmarking studies [7] where the injection kickers were set to several sets of constant amplitudes to paint hollow beams of various sizes. The wire scanner profile monitors in the RTBT extraction line showed strange results such as those shown in Fig. 10. In this figure the horizontal injection kickers were set to three different amplitudes, which ideally would paint hollow beams with three different horizontal beam sizes, with no change in the vertical beam profiles. The horizontal profiles were close to the expected shapes, but the vertical profiles showed strange shapes that were sometimes peaked rather than hollow.

The final and most direct evidence came after developing a technique [8] to recreate two dimensional real-space beam distributions at any beam position monitor in the extraction line. Single minipulses (i.e. one turn injection) are injected into the ring, the extraction time is varied, and the beam position for each extraction time is recorded. To the extent that an accumulated beam distribution is just a collection of individual beamlets from the individual injected turns (valid for non-decohering beams in the absence of space charge and other collective effects), we can achieve a fairly accurate measurement of the beam distributions, such as the one shown in Fig. 11.

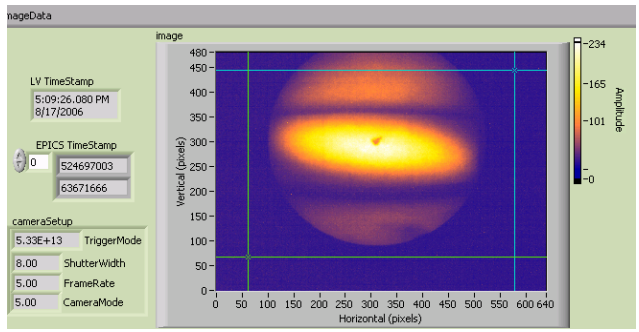

Fig. 9. An example of a beam image from the temporary view screen that was mounted to the face of the spallation target during the early stages of commissioning.

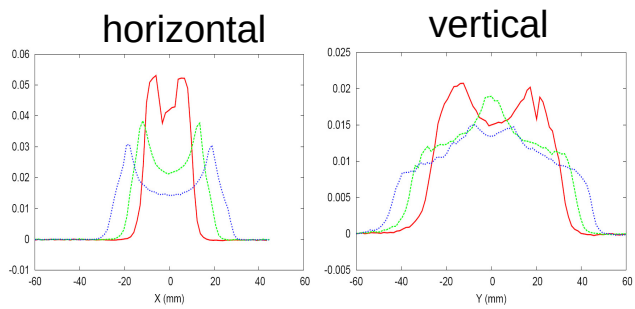

Fig. 10. Beam profiles from a wire scanner (WS20) in the RTBT extraction line, for three different horizontal injection kicker settings [7].

Based on these observations, the source of the tilted beam was eventually traced to a large skew quad component in the Lambertson septum magnet. Subsequent 3-D magnet modeling simulations [9] showed that the skew component is in fact quite large, and ORBIT simulations that include the skew quad component from the these magnet simulations give good agreement with observations. We are now in the process of investigating methods to correct the skew quad component. The best method appears to be to replace the pole tips shims in the septum magnet.

Beam diagnostics near the extraction region

The second issue in the ring extraction region is the lack of beam diagnostics. The first wire scanner is located downstream of the second quadrupole magnet in the

extraction line, and the first beam position monitor is located about 27 m downstream of the septum magnet. It is difficult to determine 14 different extraction kicker amplitudes with this limited set of diagnostics. In fact we have not yet found a set of extraction kicker amplitudes that give a good launch into the extraction line.

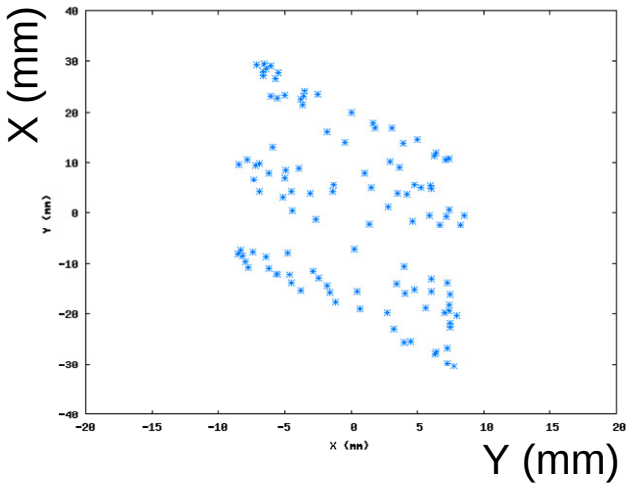

Fig. 11. A reconstructed beam distribution at a BPM (BPM25) in the RTBT extraction line [7].

Position and profile at the target

The third issue in the ring extraction region is the lack of diagnostics to measure the beam position, profile, and density at the mercury spallation target. With a final design beam power of 1.5 MW, these parameters must be measured with good accuracy [10]. However, the closest beam position or profile measurement is 9.52 m upstream of the target, as shown in Fig. 12. There is a set of thermocouples that extend into the beam halo, mounted to top, bottom, left, and right edges of the proton beam window, and located 2.1 m upstream of the target, but these only provide a rough beam position measurement.

We have developed two independent methods to measure the beam position on the target. The first is to simply equalize the top and bottom, and the left and right, halo thermocouples. This method assumes the beam halo is symmetric, and to the best of our knowledge this is in fact the case, based on the view screen measurements described earlier, and also on tests made by moving the beam left and right, and up and down, by equal amounts.

The second method is to extrapolate the beam position on the target based on the upstream beam position monitors, and apply an empirical correction factor based on measurements made while the view screen was still installed on the target (it was removed in September 2006 to allow the beam power to be increased above 10 kW). The closest BPM is 9.52 m upstream of the target. These two methods produce position measurements that differ by up to about 8 mm. This is greater than allowed position error of ±6 mm horizontal and ±4 mm vertical. We believe the halo measurement is more accurate, and so this is the method we use to center the beam on the target. If beam diagnostics were located closer to the target the accuracy of the position extrapolation method would be more accurate and more straightforward.

To measure the rms beam size on the target we first measure the rms beam sizes at the four wire scanners located 33 to 56 m upstream of the target, and at the harp located 9.5 m upstream of the target. These rms sizes are used as input to a physics application which fits an on-line optics model to the data to determine the Twiss and emittance parameters at the first wire scanner. The application then extrapolates these parameters down to the target. This method works quite well and was tested while the view screen was still installed on the target. To determine the peak beam density on the target, we first measure the beam density at the harp, and then scale the result according to the rms beam sizes at the harp and at the target. Again, if a profile measurement device was located closer to the target we could make a more accurate and straightforward measurement.

We are now working to develop a method to impregnate the steel nose of the target with chromium, which in effect will allow the target itself to be used as a view screen. This will allow the best possible beam position, size, and density measurement.

Questions and answers

Before the start of this workshop, the conveners posed three questions. The answers together with the questions follow for the case of the extraction portion of the SNS ring.

Q1: Does the system perform as expected? Did the simulations/calculations performed during the design stage accurately predict the actual performance?

A1: Except for cross plane coupling it is working as expected. We knew there were not as many diagnostics as we'd like.

Q2: What are the major limitations in performance? Were they known in the design stage?

A2: It is difficult to determine extraction kicker set points due to lack of beam position information. It is also difficult to determine the beam size, density, and position on target. We knew this in the design stage.

Q3: If someone were to begin now designing the same type of system for a similar machine, what is the one piece of advice that you would give them?

A3: Map the magnets well enough to determine the higher order multipoles, and take into account field distortion due to nearby magnets. This is especially important for large beams. Also install adequate beam diagnostics to allow easy determination of critical beam parameters

SUMMARY AND FUTURE WORK

The SNS ring injection issues are now fairly well understood. The beam loss is still several times higher than desirable. A major component of beam loss in the injection dump beam line appears to be from beam halo or

long tails on the beam distribution. We are now working to quantify the low-level beam distributions.

To further reduce the beam loss in the injection dump beam line, we are considering increasing the beam aperture for a few meters of beam line just downstream of the quadrupole magnet. To address the issue of measuring the beam position and size at the dump, we are planning to install a view screen system at the vacuum window similar to the system being developed for the target (i.e. chromium dope the vacuum window so the window itself will be the view screen).

The extraction issues are well understood. We are now working to correct the skew quadrupole component of the Lambertson septum magnet. The most promising solution seems to be to replace the pole tips shims on this magnet.

We are also working on the new view screen system for the target, to allow easy and accurate measurement of the beam distribution, position, and density at the target.

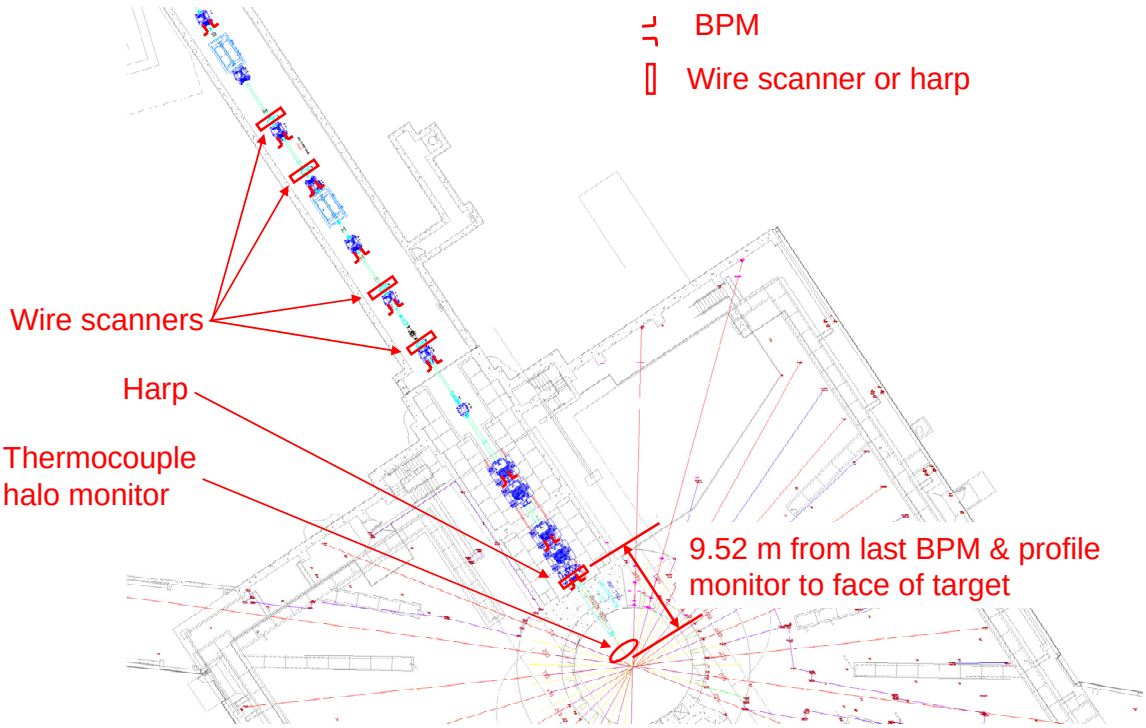

Fig. 12. Schematic diagram of the last portion of the RTBT beam line leading up to the target, showing the locations of the beam diagnostics.

ACKNOWLEDGEMENTS

I would like to acknowledge many useful discussions with Deepak Raparia. Also thanks to the SNS physics, operations, and beam instrumentation teams for many of the results presented in this paper.

REFERENCES

[1] M. Plum, Proceedings of APAC 2007, Raja Ramanna Centre for Advanced Technology(RRCAT), Indore, India, p. 6
[2] J.G. Wang and M. Plum, PRSTAB 11, 014002 (2008).
[3] J.G. Wang, EPAC 2008, p. 2389.
[4] R. Macek, Fermilab H- Transport and Injection Mini-Workshop, December 9-10, 2004.
[5] J. Holmes, private communication, August 2008.
[6] Original version of this figure from Deepak Raparia.
[7] S. Cousineau, private communication.
[8] T. Pelaia and S. Cousineau, “A Method for Constructing Transverse Real-Space Beam Distributions Using Beam Position Monitors,” to be published in NIM.
[9] J.G. Wang, proceedings of this workshop.
[10] M.A. Plum, M. Holding, and T. McManamy, proceedings of PAC 05, p. 3913.